Kinetics of the Reaction of OH with HI between 246 and 353 K

P. Campuzano-Jost[†] and J. N. Crowley*

Max-Planck-Institut für Chemie Division of Atmospheric Chemistry, Postfach 3060, 55020 Mainz, Germany

Received: November 1, 1998; In Final Form: January 28, 1999

The laser-flash photolysis technique combined with resonance fluorescence detection of OH was used to investigate the kinetics of the title reaction at temperatures between 246 and 353 K and at a total pressure of 75 ± 1 Torr Ar. Under these conditions the rate coefficient shows a negative temperature dependence which is described by $k_4(246-353\ \mathrm{K}) = 7.0^{+1.9}_{-0.4} \times 10^{-11}(T/298)^{-1.5\pm0.5}$ cm^3 s^{-1}. Both the large rate coefficient and trends in the reactivity of OH with HCl, HBr, and HI are suggestive of a reaction mechanism that proceeds without a significant activation barrier. The room temperature (294 K) rate constant is $k_4 = 6.5^{+2}_{-0.4} \times 10^{-11}$ cm^3 s^{-1}, which is significantly larger than previous measurements. Reasons for this difference and the implications of the new rate coefficients for the lifetime of HI in the atmosphere are discussed.

1. Introduction

Iodine chemistry is believed to play a role in tropospheric,[1−5] and, potentially, also stratospheric[6] ozone loss. CH_3I, which is produced by marine algae,[1] has generally been considered to be the major source of iodine in the atmosphere, although marine sources of photolabile iodo-carbons such as CH_2I_2, C_2H_5I, and CH_2ICl have recently been identified,[7,8] and which may be of a greater combined source strength than that of CH_3I. As the release of I atoms from molecules such as CH_2I_2 is facile and occurs close to the surface, the iodine chemistry of the lower troposphere may be even more important than previously assumed. Similar to bromine, I atoms are generally unreactive toward hydrocarbons and thus preferentially react with O_3. Because the major inorganic reservoir of iodine, HOI,[3] is very short lived with respect to photodissociation,[9] the presence of reactive iodine species can efficiently catalyze O_3 destruction:

$$\mathrm{I} + \mathrm{O_3} \rightarrow \mathrm{IO} + \mathrm{O_2} \quad (1)$$

$$\mathrm{IO} + \mathrm{HO_2} \rightarrow \mathrm{HOI} + \mathrm{O_2} \quad (2)$$

$$\mathrm{HOI} + h\nu \rightarrow \mathrm{I} + \mathrm{OH} \quad (3)$$

$$(\mathrm{net})\ \mathrm{HO_2} + \mathrm{O_3} \rightarrow \mathrm{OH} + 2\ \mathrm{O_2}$$

The least photolabile inorganic iodine reservoir is HI, which is formed in the reaction of I atoms with HO_2, and which is second in abundance to HOI in the lowest 2 km above the ocean.[3] The major gas-phase loss process of HI is expected to be reaction with the OH radical, which returns I atoms to the gas phase:

$$\mathrm{OH} + \mathrm{HI} \rightarrow \mathrm{H_2O} + \mathrm{I} \quad (4)$$

To date there have been three kinetic studies[10,11,12] of the reaction between OH and HI, all of which were conducted at room temperature only (≈298 K) and yield rate constants of (1.3 ± 0.5) × 10^{-11}, (2.7 ± 0.2) × 10^{-11}, and (3.3 ± 0.2) × 10^{-11} cm^3 s^{-1}, respectively. The aims of the present study were to measure the kinetics of this reaction at room temperature in order to resolve the discrepancies in the literature and to extend the temperature range to cover those relevant to atmospheric conditions.

2. Experimental Procedure

2.1. General Setup. The salient features of the present experimental setup have been given elsewhere[13] and are recounted only briefly here. The reaction took place in a thermostated, Teflon-coated stainless steel reaction vessel of ca. 150 mL volume. OH radicals were usually generated from suitable precursors by the pulsed (20 ns), unfocused light from an excimer laser. Two 8 mm irises placed before the cell define the size and shape of the laser pulse. Resonantly scattered photons from OH (excited by the emission of a microwave-powered resonance lamp) were detected by a photomultiplier that was screened by a 309 ± 5 nm interference filter. The detection limit ($S/N = 1$) is estimated as ≈1 × 10^9 OH cm^{-3} for an integration time of about 0.5 s. The temperature of the gas at the point of intersection of the laser and resonance lamp (which defines the reaction volume) was determined using a Teflon coated iron−constantan thermocouple which could be inserted into the reaction volume. The pressure was monitored using a 100 Torr capacitance manometer (MKS Baratron) with a quoted accuracy of 0.1%, and gas flows were controlled by calibrated mass-flow controllers (Tylan). The experiments were carried out using a large excess concentration of HI over OH, so that the OH decay is described by

$$[\mathrm{OH}]_t = [\mathrm{OH}]_0 \exp - \{(k_4[\mathrm{HI}] + c)t\} \quad (\mathrm{i})$$

where $[OH]_t$ is the OH concentration at time = t after the laser pulse, k_4 the bimolecular rate coefficient for the reaction of OH with HI, and c the summed rate constant for other first-order loss processes such as reaction of OH with its photolytic precursor and diffusion out of the reaction zone. The first-order decay rate constant k_{1st} was obtained by unweighted, nonlinear least-squares fitting of the OH decays and is related to the desired rate coefficient, k_4 as shown in eq ii.

$$k_{\mathrm{first}} = k_4[\mathrm{HI}] + c \quad (\mathrm{ii})$$

[†] Present address: Rosenstiel School of Marine and Atmospheric Sciences, 4600 Rickenbacker Causeway, Miami, FL 33149.

10.1021/jp984321x CCC: $18.00
Published on Web 03/23/1999

2.2. OH Source. The choice of photolytic OH precursor for kinetic experiments with HI was limited by its high reactivity and propensity to form aerosol. A number of OH sources were tested, including reactions 5, 6, 7 + 8, and 9 + 10 + 8.

$$HNO_3 + h\nu\ (248\ nm) \rightarrow OH + NO_2 \quad (5)$$

$$H_2O_2 + h\nu\ (248\ nm) \rightarrow 2\ OH \quad (6)$$

$$HI + h\nu\ (248\ nm) \rightarrow H + I \quad (7)$$

$$H + NO_2 \rightarrow OH + NO \quad (8)$$

$$NO_2 + 2h\nu\ (439.4\ nm) \rightarrow O(^1D) + NO \quad (9)$$

$$O(^1D) + H_2 \rightarrow OH + H \quad (10)$$

2.2.1. $HNO_3 + h\nu$ (248 nm). A very large increase in the scattered light from the resonance lamp could be observed when flows of HNO_3 ($\approx 1 \times 10^{15}$ cm^{-3}) and HI ($\approx 2 \times 10^{13}$ cm^{-3}) in 75 Torr Ar were mixed and introduced into the reaction vessel. This increase in scattered light in the absence of any photolytic generation of OH was attributed to aerosol formation due to reaction between these molecules. Typical scattered light signals of 700 cps (cps = counts per second) obtained for separate flows of HNO_3/Ar or HI/Ar increased to 7000−8000 cps when the flows were mixed. Efforts were made to reduce the mixing time of these two gas flows and to decrease the HNO_3 as far as possible. Even by reducing the HNO_3 concentration to 7×10^{13} cm^{-3} (with [HI] = 2×10^{13} cm^{-3}) and the contact time to ≈ 0.2 s, the measured scattered light signal was still substantial at ≈ 2000 cps. Optical absorption experiments with higher [HNO_3] and [HI] showed that the HI was quantitatively removed by reaction with HNO_3 and that condensates were observed on the walls of the absorption cell. The above observations led us to reject HNO_3 as suitable OH source.

2.2.2. HI + hν (248 nm) + NO_2 and NO_2 + 2hν + H_2/H_2O. As HI absorbs relatively strongly at 248 nm (see below), reactions 7 + 8 represent a further source of OH if NO_2 is added to the HI/Ar mixture. The concentration of OH thus generated was found to depend linearly on the HI concentration as expected and (once corrected for the background signal) its decay was exponential. However, the expected linear dependence of the pseudo-first-order rate constant k_{first} versus the concentration of HI was not obtained. We have no firm explanation for this, but note that the photolysis of HI at 248 nm to give H and I has ≈ 2 eV of excess energy, presumably mostly available as translational energy in H, which may have perturbed both the formation and reactivity of the OH product formed in reaction 8. There is evidence for an altered reactivity of vibrationally excited OH toward HBr and possibly HCl.[14]

Alternatively, the addition of NO_2 also enables the use of an OH source that has recently been developed in this laboratory,[15] the two-photon dissociation of NO_2 in the presence of H_2 (reactions 9, 10, and 8). The use of this source generated exponential decays of OH, and a linear relationship was observed between k_{first} and [HI] for [HI] < 3×10^{13} cm^{-3}. However, several observations ruled out the use of this method of OH generation. First we observed a strong dependence of the rate constant on the initial concentrations of NO_2. Room-temperature rate constants of between 1.2×10^{-10} and $\approx 5 \times 10^{-11}$ cm^3 s^{-1} could be obtained, with the lowest rate constants measured at low [NO_2].

Also, as in the HNO_3/HI experiments, an enhanced scattered light signal from the resonance lamp was observed, the size of which was dependent on the amount of NO_2 added, and on the mixing time for the HI and NO_2 flows prior to the photolysis cell. At long mixing times (t > 1s) and with concenrations of Ar (20 Torr) and H_2 ($\approx 2 \times 10^{16}$ cm^{-3}) and NO_2 (4×10^{14} cm^{-3}) a stray light signal of ≈ 20000 cps was observed. The addition of $\approx 2 \times 10^{13}$ cm^{-3} HI resulted in a signal of > 100000 cps. (These stray light values are not directly comparable to those quoted in section 2.2.1 due to a changed experimental setup). A flattening off of the stray-light signal with increasing [NO_2] indicated that HI was probably almost completely consumed in a reaction with NO_2 at high NO_2 and long mixing times. We also observed a broad absorption centered at ≈520 nm when the same concentrations of NO_2 and HI were flowed into the optical absorption cell (mixing time = 20 s) and which was absent for separate flows of HI and NO_2 in Ar. The λ_{max} of the absorption feature at 520 nm rules out that it is I_2, which absorbs with a maximum closer to 490 nm.

These observations are indicative of a thermal, dark reaction between NO_2 and HI in our experiment, which results in the formation of a product that reacts very rapidly with OH, and which has a high scattering cross section at ≈309 nm.

2.2.3. H_2O_2 + hν (248 nm). Finally, the photolysis of H_2O_2 at 248 nm proved to be the most suitable source of OH. Due to a larger absorption cross section at 248 nm than HNO_3 and a quantum yield of 2 for OH formation[16] relatively low concentrations of H_2O_2 (3×10^{14} cm^{-3}) were sufficient to generate useful OH signals. The amount of H_2O_2 was estimated from the decay rates of OH in the absence of HI, the known rate constant for OH + H_2O_2, and the typical rate constant for OH loss due to diffusion in the reactor (≈100 s^{-1} at 75 Torr).

A flowing mixture of H_2O_2 with $\approx 2 \times 10^{13}$ HI cm^{-3} caused an approximate 25% increase in the scattered light from the resonance lamp, when compared to that from flowing pure Ar. The size of the scattered light signal was however found to be unchanged upon variation of either the H_2O_2 concentration (between 1×10^{14} and 1×10^{15}) or the contact time (between 0.5 and 4 s) and similar in magnitude to that observed when HI/Ar flows were added to the cell with no H_2O_2 present.

To avoid perturbation of the OH decay via reaction 12, the OH concentration (calculated using the laser fluence at 248 nm and the H_2O_2 concentration) was kept low at $[OH]_0 \approx 5 \times 10^{11}$ cm^{-3}.

$$OH + H_2O_2 \rightarrow HO_2 + H_2O \quad (11)$$

$$OH + HO_2 \rightarrow H_2O + O_2 \quad (12)$$

The above discussion of various OH sources reveals that the addition of either NO_2 or HNO_3 to a HI/Ar mixture results in a complex chemistry that via dark, thermal reactions leads to aerosol generation, formation of other gas-phase products and loss of HI from the gas phase. Although these observations are not directly relevant to the kinetics of the reaction of OH with HI, they may provide an explanation for some of the discrepancies found in the literature data for this reaction. We shall return to this point in the discussion, where we compare our data to that obtained in both flash photolysis and discharge flow systems.

2.3. Flows and Concentrations. Extraction of the bimolecular rate coefficient for reaction of OH with HI (k_4) using eq ii requires the absolute concentration of HI in the reaction cell to be known. Gaseous HI (prepared as described below) was accurately diluted in Ar in darkened 13 L glass bulbs using 1 and 1000 Torr capacitance manometers to determine the nominal mixing ratio, which was varied between 1.3 and 2.5×10^{-4}. A

flow of HI/Ar was introduced into the reaction cell via a Kel-F needle valve which was used to vary the HI/Ar flow rate. The use of mass flow controllers and metal or Teflon needle valves proved to be nonviable for HI/Ar mixtures due to the rapid decomposition of the HI on these surfaces. Three mass flow controllers of range 10, 100, and 1000 cm^3 (STD) min^{-1} (=sccm) were used to control separate flows of Ar. The flows through the 1000 and 100 sccm controllers were directed into the photolysis cell; the flow through the 10 sccm controller passed through a bubbler containing concentrated H_2O_2 before entering the photolysis cell. Initially a flow of H_2O_2/Ar (total flow rate $\approx$ 550 sccm) was established, which, as evidenced by observations of a constant OH decay rate and signal height upon photolysis of H_2O_2 at 248 nm, took $\approx$1 h to stabilize.

Following this conditioning period, the total flow rate and the pressure in the reaction cell (100 Torr capacitance manometer) were noted. A flow of HI/Ar was added to the H_2O_2/Ar flow just before the photolysis cell and the increase in pressure noted. The total pressure was then adjusted to its original value by reducing the flow through the 100 sccm Ar controller. The change in flow through this controller then provides the equivalent flow of HI /Ar through the needle valve. This was combined with the total flow rate, the pressure in the photolysis cell, and the HI/Ar mixing ratio to yield the HI concentration. The base pressure in the absence of the HI/Ar flow was redetermined at regular intervals to check for changes in, for example, the pumping efficiency which would invalidate this method of calculating [HI]. For experiments at 75 Torr, each concentration step (around 5×10^{12} HI cm^{-3}) resulted in a pressure increase of $\approx$0.45 Torr compared to the maximum resolvable pressure change of 0.01 Torr. Drifts of greater than 0.2 Torr in the base pressure was the criterion to eliminate data. At [HI] = 5×10^{13} cm^{-3} this is just 4% of the total change in pressure due to the HI/Ar flow but is $\approx$ 25% for [HI] = 1×10^{13} cm^{-3}.

Before being mixed with the H_2O_2/Ar flows, the HI /Ar flow was passed through a glass spiral immersed in a cold bath at -110 °C. The vapor pressure of HI at this temperature is >5 Torr as verified in the present experiments on the UV spectrum of HI, whereas that of I_2 is at least 6 orders of magnitude lower. This precautionary measure should efficiently remove any I_2 impurity that may have been formed in a thermal self-reaction of HI in the darkened storage bulb or due to conditioning of the glass and Teflon tubing. As I_2 reacts extremely rapidly with OH ($k_{13} = 1.8 \times 10^{-10}$ cm^3 s^{-1} at 298 K[16]) the presence of I_2 could result in an overestimation of the rate constant.

$$OH + I_2 \rightarrow HOI + I \qquad (13)$$

As HI has a high affinity for surfaces, an additional check of the manometrically determined HI/Ar mixing ratio in the darkened storage bulb was undertaken. Following a kinetic measurement at 294 K, a well-defined fraction of the remaining contents of a HI/Ar bulb were drawn through an aqueous solution (100 mL) of 0.1 M KOH The aqueous solution was then analyzed for I^- using a freshly calibrated ion chromatograph (Dionex AS 11), and the results were compared with the expected value calculated from the nominal gas-phase mixing ratio in the glass bulb. This diagnostic test was carried out on two separate occasions and yielded on both counts a HI mixing ratio that was $\approx$20$-$25% lower than that obtained manometrically. Although it remains unclear what the source of the discrepancy might be, we note that losses of HI on the unconditioned glass tubing between the storage bulb and the KOH bubbler would result in a lower mixing ratio. Such effects would not be encountered in a kinetic experiment in which time is allowed for conditioning of glass surfaces before data is taken. Thus, although the 20$-$25% discrepancy may be regarded as an upper limit to a potential systematic overestimation of the HI concentration, in the final analysis we add an asymmetric error of +25% to our final rate constant for OH + HI at each temperature.

All experiments were carried out at a total pressure of 75 $\pm$ 1 Torr, and a total flow rate of $\approx$550 sccm, the temperature was varied between 246 and 363 K. The H_2O_2 concentration and laser fluence (per pulse at 10 Hz) were usually maintained at 3×10^{14} cm^{-3} and 8 mJ cm^{-2}, respectively, resulting in an initial OH concentration of $\approx 5 \times 10^{11}$ cm^{-3}. The HI concentration was varied between 5×10^{12} and 4.5×10^{13} cm^{-3}. Each HI/Ar mixture was used to determine a rate coefficient at room temperature and at one other temperature. This helped to eliminate systematic errors related to the mixing ratio of HI in the storage bulb that otherwise could have masked the true variation of rate coefficient with temperature.

2.4. Chemicals and Purification. Anhydrous $HNO_3(l)$ was prepared by the reaction of KNO_3 with concentrated H_2SO_4 and vacuum distilled into a cold trap at liquid N_2 temperature, before storage in the dark at -40 °C. H_2O_2 was purchased as a 70% (wht) solution in H_2O (Solvay Interox). The H_2O_2 was preconcentrated by passing Ar through it for several days. HI was prepared by drying a 55% aqueous solution (Fluka) on P_4O_{10} at 235 K, and was purified of I_2 and phosphor-iodides by repeated vacuum distillation at 163 K. NO_2 (purchased as N_2O_4, Merck, 99.5%), N_2O (Hoechst, 99.5%), and Ar (Linde, 99.999%) were used without further purification.

2.5. UV Spectrum of HI. As part of the present study, the UV spectrum of HI was determined. Initially it was anticipated that accurate optical absorption measurements of HI concentrations could supplement the determination via partial flow and pressure. However, the low concentrations of HI used resulted in optical densities that were too low to be considered reliable. The use of multireflection optics was not possible due to the rapid decomposition of HI on the metal mirror supports. In addition, the rather large volume (3 L) of our optical absorption cell meant that very long conditioning periods were required for the low HI concentrations. However, the UV spectrum of HI also enables an assessment of its loss due to photodissociation in the atmosphere, and so experiments were carried out to measure its absorption cross sections between 200 and 340 nm at room temperature. For these experiments, a quartz absorption cell of 132 cm optical path length was used. A D_2 lamp was used as source of the analysis light, which was dispersed and detected by a 0.5 m monochromator with a grating blazed at 200 nm with 300 or 600 lines/mm and a 1024 element photodiode array, respectively. To prevent formation of a adsorbed film of HI on the Suprasil quartz windows, they were heated to $\approx$50 °C. This was found necessary to obtain reproducible results in the long-wavelength tail of the HI spectrum. Pure HI was introduced into the absorption cell from its solution at $\approx$170 K which removed any I_2 impurity. The absence of any I_2 was confirmed by absorption measurements at 500 nm. Reproducible results were only obtained once the absorption cell had been preconditioned by leaving $\approx$5 Torr of HI in the cell for several minutes. Beer$-$Lambert linearity could be confirmed for seven different wavelengths between 205 and 320 nm and optical densities of up to 1.5.

3. Results

3.1. UV Absorption Spectrum of HI. The final absorption spectrum of HI is shown in Figure 1, along with previous

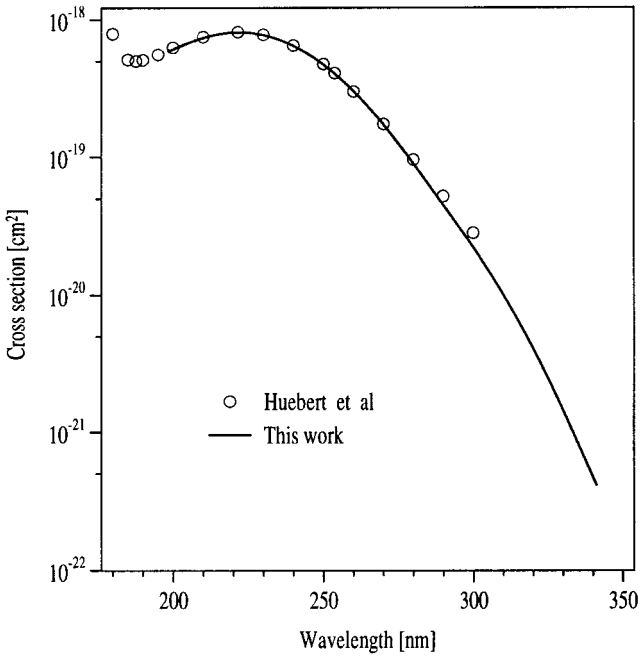

Figure 1. The UV−vis absorption cross sections of HI at 298 K. The circles are the data of Huebert et al.[17]

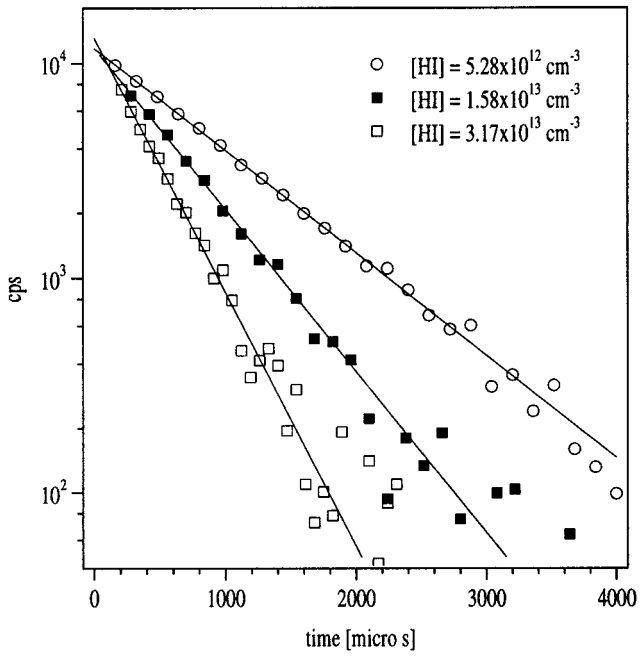

Figure 2. Exponential decays of OH in the presence of excess concentrations of HI at 294 K and a total pressure of 75 Torr Ar. The initial OH concentration was ≈5 × 10^{11} cm^{-3}. cps = counts per second.

determinations of the cross sections by Huebert et al.[17] As can be seen, there is generally good agreement in those wavelength regions where the spectra overlap. The HI spectrum consists of broad absorption features with a well-defined maximum at ≈220 nm. To the long-wavelength side of the maximum, the absorption falls approximately exponentially into the actinic region (λ > 300 nm).

3.2. Kinetics of OH + HI at Room Temperature (294 K). Figure 2 displays OH decays at 294 K obtained in various concentrations of HI. HI was always in large excess over OH, and as expected from eq i, OH decays are exponential over at least three half-lives. The slopes of such plots yield k_{1st}, which, as shown for data at 264, 294, and 354 K (Figure 3), is linearly

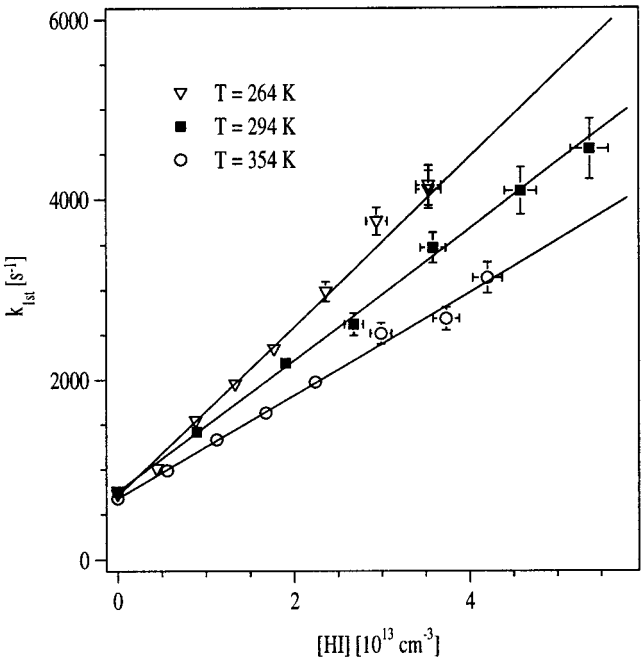

Figure 3. Plot of k_{1st} versus concentration of HI at three different temperatures and at 75 Torr Ar total pressure. The bimolecular rate coefficient each temperature is derived from the slopes (straight line fits to eq ii). The vertical error bars represent 2 σ error in k_{1st} for each [HI] and the horizontal error bars are 4% error in the estimated [HI] concentrations, which were based on observations of pressure variation in the cell during the experiment.

TABLE 1: Rate Data for OH + HI at 294 K

HI bulb	no. of decays[b]	[HI] (10^{12} cm^{-3})	k_{1st}[b] (s^{-1})	$k_4 \pm 2\sigma$[c] (10^{-11} cm^3 s^{-1})	k_4/k_4-(av)
I	7	5.69−45.5	654−3171	5.45 ± 0.12	0.83
II[a]	7	5.19−42.5	872−2850	5.78 ± 0.14	0.88
III	7	5.10−40.8	980−2869	6.53 ± 0.19	1.00
IV	7	4.53−34.0	980−2787	6.76 ± 0.26	1.04
V	6	5.28−31.7	1096−2725	6.35 ± 0.19	0.97
VI	6	5.54−24.9	1011−2197	6.60 ± 0.20	1.01
VII	6	8.43−46.4	1329−3557	6.12 ± 0.23	0.94
VIII	6	8.31−47.8	1356−4586	7.13 ± 0.43	1.09
IX	6	8.94−53.7	1416−4552	7.32 ± 0.34	1.12
X[a]	7	6.49−49.8	1442−4593	7.25 ± 0.33	1.11
all data	**65**			**6.53 ± 0.44**	

[a] Ion chromatographic tests of the HI mixing ratio were carried out on these mixtures. [b] Not counting decays in the absence of HI. [c] 2σ statistical errors including 4% error in [HI] due to pressure variation in the photolysis cell during an experiment.

dependent on [HI] (see eq ii). The room-temperature data (294 K) are summarized in Table 1.

As can be seen, a large number of decays (65) were obtained at 294 K, yielding an average rate constant of (6.53 ± 0.44) × 10^{-11} cm^{-3}. We note that the statistical errors are considerably smaller than the fluctuations in the rate constant from one HI mixture to the next, for which 294 K rate constants varied from (5.5−7.3) × 10^{-11} cm^{-3}.

3.3. Kinetics of OH + HI Between 246 and 353 K. As already mentioned, kinetic data, gathered at temperatures other than 294 K, were subject to a normalization procedure designed to eliminate apparent changes in rate coefficient with temperature that were in fact due to fluctuations in the mixing ratio of HI in its storage bulb from one experiment to the next. In Table 1 are listed the room-temperature rate constants obtained using different HI storage bulbs and, in the last column, the values of the ratio of the 294 K rate constant to the average value for all data at 294 K, which is 6.53 × 10^{-11} cm^3 s^{-1}. The inverse of

TABLE 2: Rate Data for OH + HI at Various Temperatures

temp K	HI bulb	no. of decays[a]	[HI] (10^{12} cm^{-3})	k_{1st} (s^{-1})	$k_4 \pm 2\sigma$[b] (10^{-11} cm^3 s^{-1})	k_4 (norm)[c] (10^{-11} cm^3 s^{-1})
246	VI (0.99)	8	3.98−31.8	681−3205	7.96 ± 0.25	7.88 ± 0.51
264	V (1.03)	8	4.42−35.3	1005−4153	9.41 ± 0.24	9.69 ± 0.54
272	II (1.14)	8	5.64−45.1	1033−4801	9.23 ± 0.20	10.5 ± 0.50
283	IV (0.96)	6	6.29−37.7	1692−3718	6.75 ± 0.26	6.48 ± 0.54
294	all data	65	Table 1	Table 1	Table 1	6.53 ± 0.44
315	VIII (0.92)	8	5.88−49.0	1166−4050	6.68 ± 0.35	6.14 ± 0.62
334	VII (1.06)	8	5.59−42.9	1236−3260	6.14 ± 0.24	6.51 ± 0.43
353	IX (0.89)	7	5.60−42.0	987−3135	5.75 ± 0.24	5.12 ± 0.54

[a] Excluding decays in the absence of HI. [b] 2σ statistical errors only. [c] Normalized data have been corrected for the fluctuations in the 294 K rate data for each bulb. The final errors on k_4 include errors in k_4 at 294 K (the normalization temperature).

this factor (listed in parentheses in the second column of Table 2) was then used to normalize the data at the other temperatures.

4. Discussion

4.1. Kinetics of OH with HI at 294 K. As mentioned above, the 10 individual measurements of the 294 K rate constant were carried out with different samples of HI diluted in Ar. The statistical errors (2σ) on each rate constant determination are less than 6%, whereas the reproducibility is considerably worse, with rate constant varying between (5.5 and 7.3) × 10^{-11} cm^3 s^{-1}. A number of potential systematic errors in our experimental procedure are discussed below.

The reaction between OH and I_2 is very fast ($k_{298\,K} = 1.8 \times 10^{-10}$ cm^3 s^{-1})[16] and the presence of I_2 in our HI sample could lead to an overestimation of the rate constant. The cold trap at −110 °C on the HI/Ar flow line, located a few centimeters before the mixing point with the main Ar and H_2O_2/Ar flows should however have quantitatively removed any I_2 present in the sample. This could be confirmed by analyzing the HI/Ar mixture by mass spectrometry. The ratio of signals at m/e = 127 (I^+) and 128 (HI^+) to m/e = 254 (I_2^+) exceeded 200 despite the potential for HI decomposition on metal components of the mass spectrometer. In the kinetics experiments, if any HI had decomposed to form I_2 as shown below:

$$2\,HI \rightarrow I_2 + H_2 \qquad (14)$$

and I_2 (but not H_2) is removed in the trap, then the loss of two HI molecules results in the formation of one molecule of H_2, which is relatively unreactive to OH ($k_{298\,K} = 6.7 \times 10^{-15}$ cm^3 s^{-1}).[16] The ensuing reduction in the HI-mixing ratio would result in an underestimation of the rate constant. Similarly, the mixing ratio of HI in the photolysis cell would be overestimated if HI were lost in the cold trap, once again leading to an underestimation of the rate coefficient. After a day's experiments a small amount of a pale brown deposit was observed in the cold trap, which evaporated rather quickly when warmed to room temperature. As a consequence of the method of preparation of HI, a potential impurity in the HI is PH_4I. However, this has a negligible vapor pressure below −40 °C, and thus should be removed by the distillation. A potentially more severe systematic error in our measurements is the formation of I_2 after the HI sample has passed through the −110 °C cold trap, possibly catalyzed by the presence of H_2O_2 and surfaces. Experiments were therefore carried out, in which the contact time between the H_2O_2/Ar flow and the HI/Ar flow was varied by changing the point of mixing of the two gas flows. Note that for HNO_3 and HI the same experiment in which the contact time was shortened resulted in a considerable reduction in the formation of aerosol (see experimental section). For H_2O_2/HI neither a change in the scattered light intensity from the resonance lamp nor a change in the pseudo-first-order decay rate of OH for a given H_2O_2/HI combination was observed. This observation tends to rule out that H_2O_2 and HI are interacting significantly within the contact time to influence the OH kinetics by formation of I_2 or loss of HI. After 3 h of experiments at low temperatures, the OH decay rate in the absence of HI was usually remeasured and agreed with that obtained before HI was introduced into the cell. This observation rules out any formation, storage and slow degassing of I_2 from the cold reactor walls, which would enhance the rate of removal of OH above that expected from reaction with H_2O_2 alone.

Under our experimental conditions, not only H_2O_2, but also HI is dissociated by the 248 nm excimer laser pulse. Using the absorption cross sections of HI in Figure 1, we calculate that at the high end of the HI concentration range ([HI] = 5 × 10^{13} cm^{-3}) ≈ 2.5 × 10^{11} H and I atoms cm^{-3} are generated along with the ≈5 × 10^{11} OH cm^{-3}. At lower HI concentrations the ratio of OH to H or I is much larger. A potential perturbation of the OH kinetics arises if H atoms can react with H_2O_2 to regenerate OH and also HO_2:

$$H + H_2O_2 \rightarrow OH + HO_2 \qquad (15)$$

$$H + HO_2 \rightarrow 2\,OH \qquad (16)$$

However, the rate constant for H + H_2O_2 is very low ($k_{15} = 4 \times 10^{-14}$ cm^3 s^{-1}) and results in an initial OH reformation rate of just 12 s^{-1} for [H_2O_2] = 3 × 10^{14} cm^{-3} compared to decay rate of up to 4000 s^{-1}. Alternatively, the reaction of H atoms with O_2 impurity (which may be formed in the thermal decomposition of H_2O_2) can form HO_2, which may react as above to form OH. By analogy with OH + Br, the reaction of I atoms with OH is expected to be too slow to perturb the OH decays significantly. In addition to the above considerations, a detailed analysis of the influence of these reactions, and others resulting from the simultaneous formation of OH, I, and H in roughly equal concentrations, was made by numerical simulation[18] of the reaction scheme outlined in Table 3. The results of the simulation (Figure 4) show that in the "worst case" scenario, high laser fluence and high [HI] (see figure caption for details), the OH profile is perturbed only slightly from the expected exponential decay. A sensitivity analysis showed that in the absence of I_2 impurity, the modeled decay rate was reduced by ≈1.5% when compared to that expected on the basis of reaction of OH with H_2O_2 and HI alone. The addition of a 1% I_2 impurity is expected to increase the decay rate by ≈2.5% over that obtained from reaction with HI and H_2O_2 alone. When this I_2 impurity was modeled with complete chemistry, the increase in decay rate was modified to just +1%.

Thus, under our normal experimental conditions, we conclude that none of the modeled secondary chemistry was able to influence the OH decays significantly. To confirm this experimentally, OH decays were measured in which the laser fluence

TABLE 3: Chemical Scheme Used in Numerical Simulations

reaction	k(298 K, 100 Torr) [cm^3 s^{-1}]	ref
$H_2O_2 + h\nu \rightarrow 2$ OH		16 (cross sections)
$HI + h\nu \rightarrow H + I$		this work (cross sections)
$OH + H_2O_2 \rightarrow HO_2 + H_2O$	1.7×10^{-12}	16
$OH + HI \rightarrow I + H_2O$	6.0×10^{-11}	this work
$OH + HO_2 \rightarrow O_2 + H_2O$	1.1×10^{-10}	16
$OH + I_2 \rightarrow HOI + I$	1.8×10^{-10}	16
$OH + HOI \rightarrow H_2O + OI$	2×10^{-10}	estimated[a]
$HO_2 + HO_2 \rightarrow H_2O_2 + O_2$	1.7×10^{-12}	16
$OH + OH \rightarrow H_2O_2$	2.0×10^{-12}	16
$I + I \rightarrow I_2$	3.0×10^{-13}	27
$I + HO_2 \rightarrow HI + O_2$	3.8×10^{-13}	16
$H + HI \rightarrow H_2 + I$	2×10^{-11}	28, 29
$H + H_2O_2 \rightarrow OH + H_2O$	4.0×10^{-14}	30
$I + H_2O_2 \rightarrow HI + HO_2$	$< 5 \times 10^{-16}$	estimated[b]
$H + HO_2 \rightarrow OH + OH$	7.2×10^{-11}	31
$H + I_2 \rightarrow HI + I$	6.2×10^{-10}	29
$H + O_2 \rightarrow HO_2$	2.0×10^{-13}	16, note c
$H + OH \rightarrow H_2O$	4.0×10^{-13}	32

[a] Estimated upper limit. [b] By comparison to $Br + H_2O_2$. [c] The main source of O_2 was the decomposition of H_2O_2. Initial concentrations of OH, H atoms, and I atoms were calculated from the laser fluence and the H_2O_2 and HI concentrations, respectively. The H_2O_2 concentration was calculated via the OH decay rate in the absence of HI (see text).

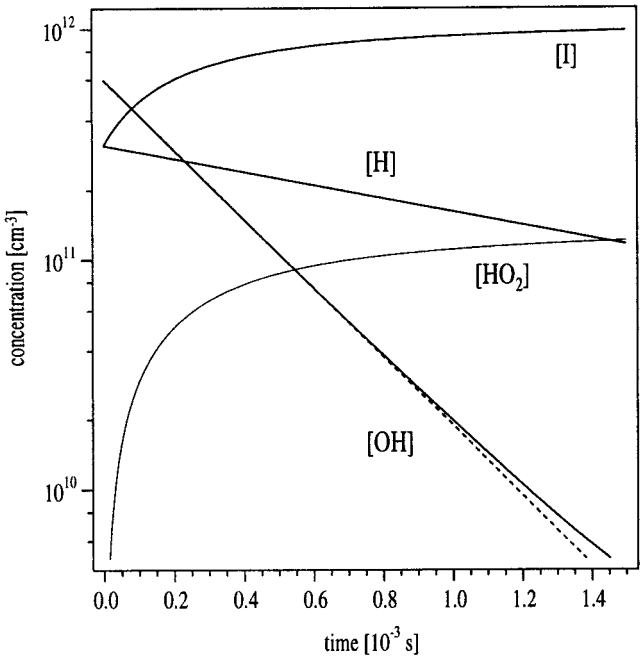

Figure 4. Calculated concentration profiles for OH, and other important species in the photolysis of H_2O_2 (3×10^{14} cm^{-3}), and HI (5×10^{13} cm^{-3}). The 248 nm laser fluence (per pulse) was 10 mJ cm^{-2}, $T = 294$ K, the total pressure was 75 Torr Ar. The chemistry modeled in the calculation is listed in Table 3. The solid lines are derived from chemical modeling, the dotted line is the calculated, nonperturbed exponential decay of OH due to reaction with HI and H_2O_2 only.

was increased by up to 30 mJ cm^{-2} which resulted in an increase by about a factor of 3−4 in the initial radical concentrations (including H and I). Even under these conditions, no dependence of reaction rates on the laser energy could be observed.

The preferred explanation for the scatter in the rate constant at 294 K is a systematic error in the HI mixing ratio. The accurate preparation of diluted samples of HI in Ar with HI partial pressures of only 200 mTorr is difficult due to its affinity for surfaces. As noted in the UV absorption experiments, conditioned glass surfaces were necessary to get reproducible results, even at high pressures of HI. Our ion chromatographic spot checks on two samples indicated a deviation of $\approx -20\%$ and -25% from that expected. As the experimental procedure was the same for the preparation of each HI storage bulb we assume that any variation in HI is statistical, and therefore take an average of the 10 determinations at 294 K to derive a rate constant of $k_4 = (6.53 \pm 0.44) \times 10^{-11}$ cm^3 s^{-1}. Considering the ≈25% deviation in IC measurement as a potential systematic error we derive a final value of $k_4 = 6.5^{+2}_{-0.4} \times 10^{-11}$ cm^3 s^{-1} at 294 K.

We now compare our 294 K rate constant to other determinations. Takacs and Glass[10] used the discharge flow method with EPR detection of OH to measure the kinetics of the reaction at 298 K. As discussed by these authors, a low sensitivity to OH in their experiment resulted in poor spatial resolution in the flow tube, resulting in inaccuracies in the rate constant, which they measured as $(1.3 \pm 0.5) \times 10^{-11}$ cm^3 s^{-1}. As noted by Mac Leod et al.,[11] the same experimental setup was used by Takacs and Glass to measure a rate constant for OH + HBr which has since been shown to be too low by a factor of 2. Another discharge flow/EPR study of this reaction was undertaken by Lancar et al.,[12] who, with improved OH sensitivity, derived a rate constant of $(3.3 \pm 0.2) \times 10^{-11}$ cm^3 s^{-1}. These authors occasionally employed a cold trap at 250 K to remove any I_2 impurity from their HI /He flow but noted that it had no effect on the rate constant.

At the same time, and in the same research group, experiments were carried out using the laser−photolysis resonance fluorescence technique (Mac Leod et al.[11]), which yielded a rate constant of $(2.7 \pm 0.2) \times 10^{-11}$ cm^3 s^{-1} at 298 K. We note that in the experiments of Mac Leod et al.[11] the 248 nm photolysis of $\approx 7 \times 10^{14}$ HNO_3 cm^{-3} was used to generate $(2-4) \times 10^{11}$ cm^{-3} OH. As we discussed earlier, the mixing of HNO_3 and HI in our experiments under similar conditions resulted in aerosol formation, as shown by enhanced scattered light from the resonance lamp, and for higher HNO_3 in total removal of the HI from the gas phase. From Figure 2 of Mac Leod et al.[11] it is apparent that the signal from OH (laser on) is only a factor of 3 greater than the background signal when HNO_3 and HI flows were present, but the laser was disabled. As the background signal in the absence of HI was not reported in this work we cannot infer if the relatively high scattered light signal is enhanced due to aerosol formation. In our experiment, in the absence of aerosol, the ratio of OH signal to background signal was ≈20 for $[OH]_i = 5 \times 10^{11}$ cm^{-3}. Any loss of HI via reaction with HNO_3 would result in an underestimated rate constant for OH + HI. Further, Mac Leod et al.[11] draw attention to an anomaly in their second-order plot of k_{first} versus [HI]. The measured loss rate of OH in the absence of HI was 150 ± 30 s^{-1}, compared to an extrapolated intercept on the ordinate of 284 ± 42 s^{-1} in the presence of HI, indicating some curvature in the data, and possibly that the rate constant is underestimated.

The difference between the room-temperature rate constant of Mac Leod et al. and the present study are thus probably explained by the use of different OH precursors. Using the same conditions as Mac Leod et al., we were unable to gather useful data for the reaction of OH + HI. Explanations for the different rate constant between the present result and the discharge flow study of Lancar et al. are more difficult to find. We note however, that the OH source used was the reaction of H-atoms with NO_2. We have shown that the mixing of HI and NO_2 can also be problematic and lead to aerosol formation (i.e., to loss of HI). However, under our conditions, the mixing time for the separate HI/Ar and NO_2/Ar flows in the inlet to the photolysis

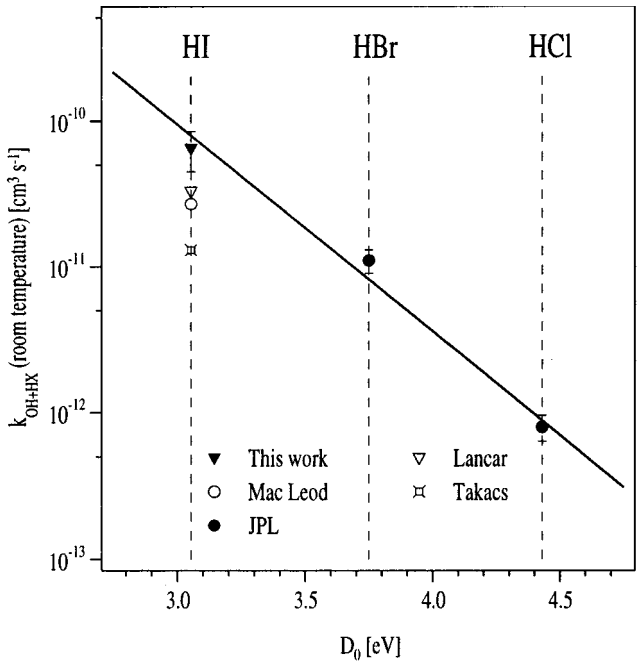

Figure 5. Room-temperature rate constant for OH + HX (this work at 294 K, Lancar,[12] Mac Leod,[11] and Takacs[10] at 298 K) versus binding energy of H−X, where X = Cl, Br, and I. The OH + HCl and OH + HBr data are taken from the most recent recommendation (JPL).[16]

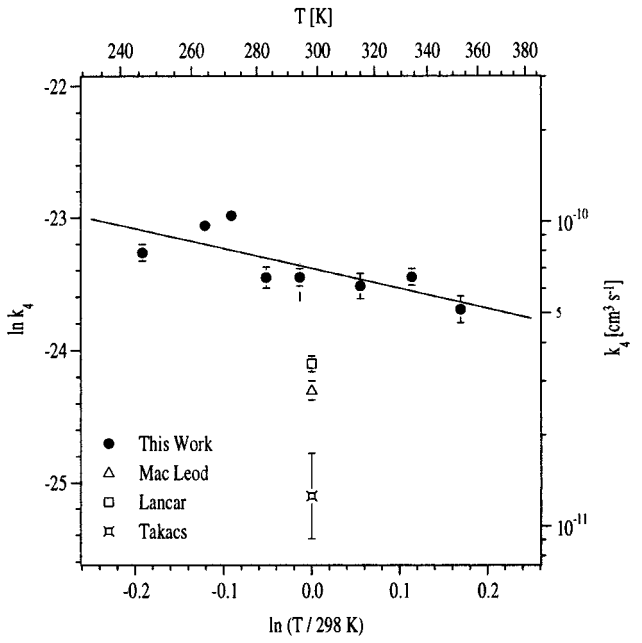

Figure 6. Temperature dependence of the rate coefficient for OH + HI. Error bars are 2σ. The vertical line at 294 K covers the total scatter in k(294 K) between 5.45 × 10^{-11} and 7.32 × 10^{-11} cm^3 s^{-1}. Also shown are the data for OH + HI from Lancar,[12] Mac Leod,[11] and Takacs.[10]

cell was about 2 s, whereas the mixing time in the discharge flow experiment was of the order of 0.1 s or less, and our observations are not necessarily applicable. We also note that the scheme for OH generation used by these authors produces vibrationally excited OH,[19] which is inefficiently quenched by 1 Torr of He used as buffer gas.[20] It is very possible that vibrational excitation in OH may manifest itself as a reduction in the rate coefficient for reaction with HI (see discussion).

In Figure 5 we plot the room-temperature rate constants from this work and those of Takacs and Glass, Mac Leod et al., and Lancar et al. versus the bond energy of HI, and also data for HBr and HCl. As can be seen the rate constant correlates reasonably well with the bond energy of HX, indicating that the reaction proceeds (mainly) via H atom abstraction.

4.2. Temperature-Dependent Rate Coefficients. Figure 6 displays the data at all temperatures. Only the average value for 294 K is shown along with a vertical line that encompasses the spread of results at this temperature. Despite the scatter in the data the rate coefficient clearly displays a slight negative temperature dependence. We emphasize again that due to the normalization procedure, whereby each rate coefficient is measured relative to one at room temperature, the slight increase in rate coefficient with decreasing temperature is not due to an experimental artifact associated with mixing ratio errors in HI. Also, even without the normalization, the trend in rate coefficient with temperature is negative.

The rate coefficient is given by

$$k_4\,(246-353\ \mathrm{K}) = 7.0^{+1.9}_{-0.4} \times 10^{-11}(T/298)^{-1.5\pm0.5}\ \mathrm{cm^3\ s^{-1}}$$

A negative temperature dependence is frequently observed when a reaction proceeds via formation of an association complex, which is more readily stabilized at low temperatures and higher pressures. In such a case, neither a large rate coefficient for a radical−molecule reaction nor the observed good correlation between the room temperature rate constant and the bond energy are expected. For the reaction of OH with HI, the negative temperature dependence is more likely related to a temperature-dependent preexponential factor. Due to the low bond energy of H−I and its high polarizability there is not expected to be a significant activation barrier to reaction with OH, and the T^{-n} temperature dependence of the rate coefficient may be expected.

The present result of a $T^{-(1.5\,\pm\,0.5)}$ temperature dependence for OH + HI may be compared to the reaction of OH with HBr, which has been shown to have no significant activation barrier between 249 and 416 K[21] but a rate coefficient that increases monotonically with decreasing temperature between 295 and 23 K is described by a $T^{(-0.86\,\pm\,0.1)}$ temperature dependence[22] and which is decreased when OH (v = 0) is vibrationally excited, OH (v = 1).[14] For OH + HCl a positive activation barrier of 2.9 kJ mol^{-1} is observed[16] continuing the trend of increasingly positive T dependencies for HI, HBr, and HCl.

We can also compare our results with the rapid reaction of Cl atoms with HI ($k_{295} \approx 1.5 \times 10^{-10}$ cm^3 s^{-1})[23,24] which displays a complex temperature dependence with the rate coefficient decreasing with increasing temperature above ≈ 300 K and displaying the reverse behavior at t < 300 K.[23] In addition, the ratio of rate coefficient for Cl atoms with HI and DI also showed a pronounced temperature dependence and an increase in the translational energy of the Cl atom reduced the rate coefficient. These results were interpreted in terms of a complex reaction mechanism in which the Cl atoms is first attracted to the I end of HI prior to a H rotation to give the HCl and I products.[25] Vibrational excitation in OH may lead to similar effects. Our present results do not enable us to draw conclusions regarding the detailed mechanism of the reaction between OH and HI, and we note that experiments using deuterated analogues of HI and OH would be useful in this respect.

4.3. Atmospheric Lifetime of HI. In this section we examine relative efficiencies of the various gas-phase loss processes for HI in the atmosphere. Assuming an OH concentration of 5 × 10^6 cm^{-3}, representative for the sunlit troposphere and lower

stratosphere at mid-latitudes, we calculate the loss rate of HI of $\approx 3 \times 10^{-4}$ s^{-1}, resulting in a lifetime of close to 1 h with respect to removal by OH. To assess the contribution of photolysis of HI to its overall loss in the atmosphere, *J* value calculations[26] were performed using the UV spectrum presented in Figure 1 and assuming a quantum yield of unity. The *J* value was found to be 1×10^{-5} s^{-1} at the surface, increasing to 2×10^{-5} at an altitude of 10−20 km and zenith angles of 40°. This is clearly too slow to compete with reaction with OH, which represents the dominant loss process for HI throughout the atmosphere.

5. Conclusions

Rate coefficients for the reaction of OH with HI were obtained at 75 Torr and at temperatures between 246 and 253 K. The rate coefficient displays a negative temperature dependence in this range, k_4 (246−353 K) $= 7.0^{+1.9}_{-0.4} \times 10^{-11}(T/298)^{-1.5\pm0.5}$ cm^3 s^{-1}, and is a factor of ≈2 greater than previous determinations at room temperature. At OH concentrations of $\approx 5 \times 10^6$ cm^{-3} this expression results in a lifetime for HI of ≈1 h. As part of this study the UV absorption cross sections of HI were also determined which allowed the calculation of the lifetime of atmospheric HI with respect to photodissociation as ≈18 h.

Acknowledgment. We thank the European community for financial support (Grant ENV4-CT95-0013, LEXIS), and Jochen Landgraf for the *J* value calculations.

References and Notes

(1) Chameides, W. L.; Davis, D. *J. Geophys. Res.* **1980**, *85*, 7383.
(2) Chatfield, R. B.; Crutzen, P. J. *J. Geophys. Res.* **1990**, *95*, 22319.
(3) Davis, D.; Crawford, J.; Liu, S.; McKeen, S.; Bandy, A.; Thornton, D.; Rowland, F.; Blake, D. *J. Geophys. Res.* **1996**, *101*, 2135.
(4) Jenkin, M. E.; Cox, R. A.; Candeland, D. E. *J. Atmos. Chem.* **1985**, *2*, 359.
(5) Jenkin, M. E. *NATO ASI Ser*. **1993**, *I7*, 405.
(6) Solomon, S.; Garcia, R. R.; Ravishankara, A. R. *J. Geophys. Res.* **1994**, *99*, 20491.
(7) Yokouchi, Y.; Mukai, H.; Yamamoto, H.; Otsuki, A.; Saitoh, C.; Nojiri, Y. *J. Geophys. Res.* **1997**, *102*, 8805.
(8) Carpenter, L. J.; Sturges, W. T.; Penkett, S. A.; Liss, P. S.; Alicke, B.; Hebestreit, K.; Platt, U. *J. Geophys. Res.* **1998**. Manuscript submitted for publication.
(9) Bauer, D.; Ingham, T.; Carl, S. A.; Moortgat, G. K.; Crowley, J. N. *J. Phys. Chem.* **1998**, *102*, 2857.
(10) Takacs, G. A.; Glass, G. P. *J. Phys. Chem.* **1973**, *77*, 1948.
(11) MacLeod, H.; Balestra, C.; Jourdian, J. L.; Laverdet, G.; LeBras, G. *Int. J. Chem. Kinet.* **1990**, *22*, 1167.
(12) Lancar, I. T.; Mellouki, A.; Poulet, G. *Chem. Phys. Lett.* **1991**, *177*, 554.
(13) Crowley, J. N.; Campuzano-Jost, P.; Moortgat, G. K. *J. Phys. Chem.* **1996**, *100*, 3601.
(14) Cannon, B. D.; Robertshaw, J. S.; Smith, I. W. M.; Williams, M. D. *Chem. Phys. Lett.* **1984**, *105*.
(15) Carl, S. A.; Crowley, J. N. *J. Phys. Chem.* **1998**, *102*, 8131.
(16) DeMore, W. B.; Sander, S. P.; Golden, D. M.; Hampson, R. F.; Kurylo, M. J.; Howard, C. J.; Ravishankara, A. R.; Kolb, C. E.; Molina, M. J. Chemical Kinetics and Photochemical data for use in stratospheric modelling. JPL Publication 97-4; Jet Propulsion Laboratory: Pasadena, 1997.
(17) Huebert, B. J.; Martin, R. M. *J. Phys. Chem.* **1968**, *72*, 3046.
(18) Curtis, A. R.; Sweetenham, W. P. FACSIMILE release H user's manual. AERE report R11771; HMSO, London, 1987).
(19) Silver, J. A.; Dimpfl, W. L.; Brophy, J. H.; Kinsey, J. L. *J. Chem. Phys.* **1976**, *65*, 1811.
(20) Rensberger, K. J.; Jeffries, J. B.; Crosley, D. R. *J. Chem. Phys.* **1989**, *90*, 2174.
(21) Ravishankara, A. R.; Wine, P. H.; Langford, A. O. *Chem. Phys. Lett.* **1979**, *63*, 479.
(22) Sims, I. R.; Smith, I. W. M.; Clary, D. C.; Bocherel, P.; Rowe, B. R. *J. Chem. Phys.* **1994**, *101*, 1748.
(23) Mei, C.-C.; Moore, C. B. *J. Chem. Phys.* **1977**, *67*, 3936.
(24) Dolson, D. A.; Leone, S. R. *J. Chem. Phys.* **1982**, *77*, 4009.
(25) Mei, C.-C.; Moore, C. B. *J. Chem. Phys.* **1979**, *70*, 1759.
(26) Landgraf, J.; Crutzen, P. J. *J. Atmos. Sci.* **1997**. In press.
(27) Baulch, D. L.; Duxbury. J.; Grant, S. J.; Montague, D. C. *J. Phys. Chem. Ref. Data* **1981**, *10*, 1.
(28) Umemoto, H.; Nakagawa, S.; Tsunashima, S.; Sato, S. *J. Chem. Phys.* **1988**, *124*, 259.
(29) Lorenz, K.; Wagner, H. G.; Zellner, R. *Ber. Bunsen-Ges. Phys. Chem.* **1979**, *83*, 556.
(30) Atkinson, R.; Baulch, D. L.; Cox, R. A.; Hampson, R. F.; Kerr, J. A.; Troe, J. *J. Phys. Chem. Ref. Data* **1992**, *21*, 1125.
(31) Baulch, D. L.; Cobos, C. J.; Cox, R. A.; Esser, C.; Frank, P.; Just, Th.; Kerr, J. A.; Pilling, M. J.; Troe, J.; Walker, R. W.; Warnatz, J. *J. Phys. Chem. Ref. Data*, **1992**, *21*, 411.
(32) Tsang, W.; Hampson, R. F. *J. Phys. Chem. Ref. Data* **1996,** *15*, 1087.